Ammonolysis and Aminolysis of β-Lactams: A Theoretical Study

Natalia Díaz, Dimas Suárez, and Tomás L. Sordo*[a]

Abstract: The ring opening of 2-azetidinone through neutral ammonolysis and aminolysis processes was studied by means of different quantum chemical methods (MP2/6-31G**, B3LYP/6-31G**, and G2(MP2,SVP) levels of theory) as a first step to the theoretical understanding of the aminolysis reaction of β-lactam antibiotics. The exploration of the corresponding potential energy surfaces renders two different mechanistic routes for both ammonolysis and aminolysis processes: a concerted pathway through a 1,2 addition of the H–NRH bond to the amide C–N bond, and a stepwise one through several tetrahedral intermediates. In the case of the stepwise mechanism, the *syn* periplanar orientation of the attacking NH_2R with respect to the lone pair of the amidic nitrogen atom is more favorable than the *anti* one. The G2(MP2,SVP) level predicts that the nonconcerted route is the most favored one presenting a rate-determining energy barrier with respect to the corresponding prereactive complexes of 47.3 kcal mol^{-1} and 41.3 kcal mol^{-1} for ammonolysis and aminolysis reactions of 2-azetidinone, respectively. The kinetic and thermodynamic role of strain energy in 2-azetidinone is also discussed by comparison with the corresponding energy profile for the ammonolysis of *N*-methylacetamide. For aminolysis, the electrostatic effect of solvent evaluated at the MP2/6-31G** SCRF level tends to stabilize the stepwise transition structures with respect to the concerted one.

Keywords: ab initio calculations · aminolysis · ammonolysis · lactams · strain energy

Introduction

The major antigenic determinant of penicillin allergy is the penicilloyl group bound by an amide linkage to ε-amino-groups of lysine residues in proteins[1, 2] like human serum albumin.[1e–1f] On the other hand, the aminolysis reaction is also of interest because the bacterial enzyme inhibited by β-lactam antibiotics catalyzes a transpeptidation reaction that closes the peptide cross-bridges, which stabilize the peptidoglycan, a cross-linked polymer which completely surrounds the cell.

The aminolysis of the β-lactam antibiotics is a substitution reaction in which an acyl group is transferred from one amino group to another. A proton has to be removed from the attacking amine and a proton has to be added to the leaving amino group. These kinds of processes, which normally are difficult because of the small free-energy change associated with them, occur readily with β-lactams.[3] Ring opening in β-lactams is accompanied by a large release of strain energy, which makes the reaction thermodynamically feasible. However, it has also been reported that the rates of ring opening of β-lactams are not exceptional compared with the total strain energy involved.[3]

The aminolysis of penicillins and cephalosporins is a stepwise process catalyzed predominantly by bases, which remove a proton from the attacking amine. There is kinetic evidence for the reversible formation of a tetrahedral intermediate[1a] in the amine-assisted reaction. In the experimental study of the aminolysis of benzylpenicillin in aqueous solutions of the amine, it has been found that the importance of the different terms contributing to the observed pseudo-first-order rate constant for the disappearance of the penicillin depends on the basicity and concentration of the amine and the pH.[1a] Particularly interesting are the kinetic terms corresponding to the uncatalyzed and the amine-catalyzed aminolysis pathways, which are the predominant terms when weakly basic amines are employed in the biologically relevant region pH 6–8. In contrast, the rate constants for the amine-catalyzed reactions of strongly basic amines become more important with increasing concentrations of amine, while the rate constants for the uncatalyzed reactions of basic monoamines contribute little to the observed rate and are difficult to determine accurately.

In the present work we have studied, using quantum chemical methods, the uncatalyzed ring opening of 2-azetidi-

[a] Dr. T. L. Sordo, N. Díaz, Dr. D. Suárez
Departamento de Química Física y Analítica
Facultad de Química, Universidad de Oviedo, C/ Julián Clavería 8
E-33006 Oviedo, Principado de Asturias (Spain)
Fax: (+349) 85103125
E-mail: tsg@dwarf1.quimica.uniovi.es

Supporting information for this contribution is available on the WWW under http://www.wiley-vch.de/home/chemistry/. This includes Figure S1 which displays the optimized geometry of the critical structures located along the reaction coordinate for the ammonolysis of *N*-methylacetamide, and Table S1 which presents the corresponding relative energies.

  0947-6539/99/0503-1045 $ 17.50+.50/0

none by the reaction with NH_3 (ammonolysis) and CH_3NH_2 (aminolysis) as a first step in the understanding of the aminolysis reaction of β-lactam antibiotics. The different reaction paths through which the acyl group and the proton are transferred from one amino group to the other are investigated. A comparative study of the ammonolysis of an open-chain amide (*N*-methylacetamide) will be carried out in order to determine the role of the strain of the β-lactam ring in the mechanism of the process. The electrostatic effect of solvent on the different reaction paths for the aminolysis of 2-azetidinone will be taken into account.

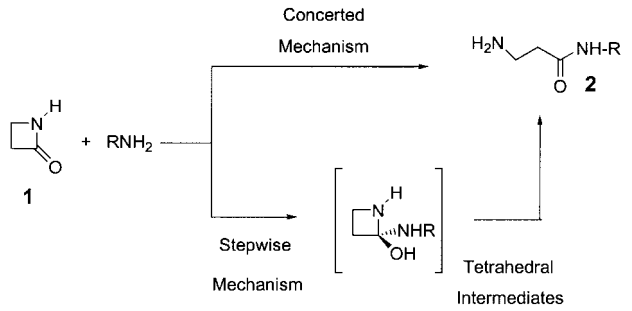

Scheme 1. Two possible pathways for ammonolysis and aminolysis.

Computational Methods

Ab initio calculations were carried out with the G94 program system[4] in which extra links for the solvent effect treatment have been added.[5] Preliminary exploration of the potential energy surfaces (PES) studied in this work was carried out at the HF/6-31G* level. Stable structures were fully optimized and transition structures (TS) relocated by means of the Schlegel algorithm[6] at the MP2(FC)/6-31G** and B3LYP/6-31G** levels.[7–9] All the critical points were further characterized by analytic computation of harmonic frequencies at B3LYP/6-31G** level.

In order to estimate the effect of larger basis sets and more elaborated *N*-electron treatments on the relative energies for the ammonolysis process, electronic energies were also computed for the MP2/6-31G** optimized structures by means of the G2(MP2,SVP) scheme,[10] which approximates the QCISD(T)/6-311 + G(3df,2p) level in an additive fashion as given in Equation (1). Analogously, B3LYP/6-311 + G(3df,2p) single point calculations were carried out on all the B3LYP/6-31G** optimized structures.

$$E[\text{QCISD(T)/6-311+G(3df,2p)}] \approx E[\text{G2(MP2,SVP)}] = E[\text{QCISD(T)/6-31G*}] + E[\text{MP2/6-311+G(3df,2p)}] - E[\text{MP2/6-31G*}] \quad (1)$$

Quantum chemical computations on solvated molecules and TSs were carried out with a general self-consistent reaction field (SCRF) model[11] at the MP2/6-31G** theory level. The solvent is represented by a continuum characterized by its relative static dielectric permittivity, ε. The solute, which is placed in a cavity created in the continuum, after spending some cavitation energy polarizes the continuum, which in turn creates an electric field inside the cavity. Once the equilibrium is reached, the electrostatic part of the free energy corresponding to the solvation process is obtained by means of a monocentric multipolar expansion of the molecular charge distribution.[12] The SCRF continuum model employed assumes a general cavity shape that is obtained from van der Waals solute atomic spheres with modified radii ($1.3084\,r_{vdW}$),[11a] necessary to fullfil the volume condition. A relative permittivity of 78.3 was used to simulate water as the solvent used in the experimental work.

The main B3LYP/6-31G** TSs were analyzed by means of a population analysis carried out by expanding the molecular orbitals (MO) of a complex system, in terms of the MOs of its fragments (using the geometry of each fragment in the corresponding transition structures) thus allowing a more detailed characterization of the electronic interactions between reactants.[13] In addition, B3LYP/6-31G** energy barriers were broken down into two main contributions, namely, the energy of geometrical distortion and the energy of interaction between the distorted fragments in order to account separately for the geometrical and electronic characteristics of the corresponding TSs.[14] This analyses were performed using a revised version of the ANACAL program.[15]

Results and Discussion

The exploration of the PES corresponding to the neutral ammonolysis and aminolysis of 2-azetidinone renders two possible pathways for both processes (see Scheme 1). The first mechanism corresponds to the concerted 1,2 addition of the H–NRH bond to the amide C–N bond, involving the simultaneous rupture of the β-lactam ring **1** and the transfer of the hydrogen atom to the leaving amine group. The second mechanistic route proceeds in a stepwise manner involving several tetrahedral intermediates, which are formed as a result of the addition of the H–NRH bond across the carbonyl double bond of the amide, with the transfer of the hydrogen atom to the carbonylic oxygen atom. One of these intermediates can evolve through a TS for 1,3-hydrogen shift, which implies the simultaneous breaking of the endocyclic C–N bond rendering thus the final product **2**. Analogous mechanistic routes have been previously found in theoretical studies of the neutral hydrolysis of amides[16–18] and azetidinones.[19–20]

We present first the results for the ammnolysis reaction of 2-azetidinone and *N*-methylacetamide, discussing the effect of the ring strain in the mechanism, and then the results for the aminolysis of 2-azetidinone taking into account the electrostatic effect of solvent.

Ammonolysis reactions of 2-azetidinone and *N*-methylacetamide: The optimized geometries of the structures located along the concerted and stepwise reaction paths for the gas-phase ammonolysis of 2-azetidinone are shown in Figure 1. Table 1 displays the corresponding relative energies obtained at the different theory levels employed in this work including the ZPVE correction from the B3LYP/6-31G** unscaled frequencies.

Concerted mechanism: According to intrinsic reaction coordinate[21] (IRC) calculations at the HF/6-31G* level, as well as the exploration on the PES carried out at the correlated levels of theory, the first critical structure located along both the concerted and stepwise reaction paths for the ammonolysis of 2-azetidinone is the intermolecular complex between ammonia and β-lactam **CA** shown in Figure 1. This complex, which is similar to the one found in the theoretical study of hydrolysis of *N*-methylazetidinone,[20] presents a typical O···HN hydrogen bond, having an equilibrium distance of around 2.2 Å, and a weak N···HC hydrogen bond whose equilibrium distance is 2.7 Å. The binding energy is quite similar at the MP2/6-31G** and B3LYP/6-31G** levels of theory: -4.5 kcal mol^{-1} and -4.0 kcal mol^{-1}, respectively.

The TS for the concerted ammonolysis process corresponds to the 1,2 addition of H–NH_2 to the C–N amide bond (**TS_cA** in Figure 1) in which the attacking ammonia molecule is *syn* periplanar to the nitrogen lone pair at 2-azetidinone. **TS_cA** resembles closely the TSs computed for the addition of

0947-6539/99/0503-1046 $ 17.50+.50/0 *Chem. Eur. J.* **1999**, *5*, No. 3

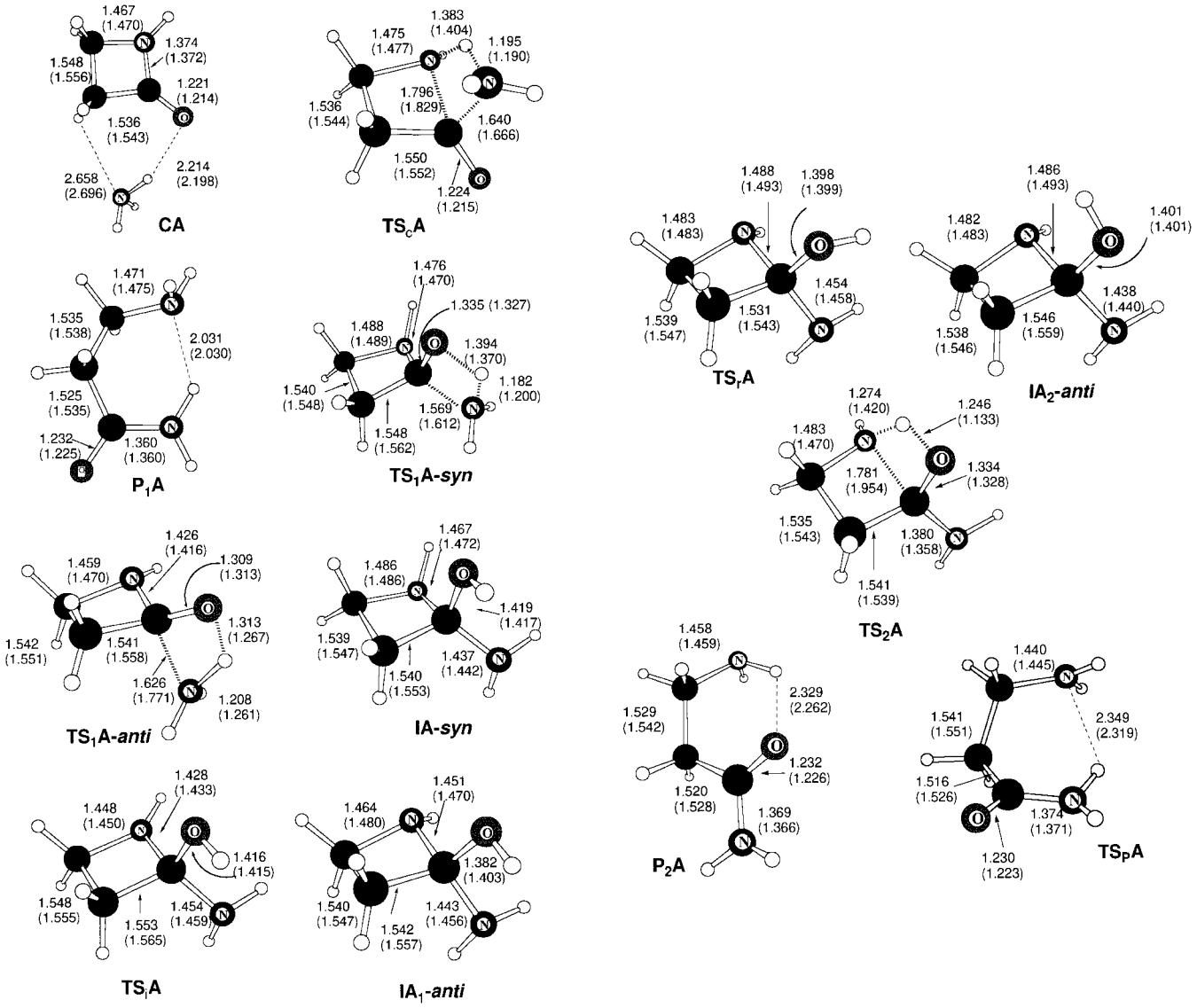

Figure 1. MP2/6-31G**-optimized structures for the ammonolysis reaction of 2-azetidinone. Distances in Å. B3LYP/6-31G** values are in parentheses.

Table 1. Relative energies[a] [kcal mol^{-1}] with respect to reactants of the structures considered in the ammonolysis reaction of 2-azetidinone.

	MP2/6-31G**	G2(MP2,SVP)[b]	B3LYP/6-31G**	B3LYP/6-311 + G(3df,2p)[c]
NH_3+2-azetidinone	0.0	0.0	0.0	0.0
CA	− 4.5	− 3.3	− 4.0	− 1.6
TS$_c$A	43.1	46.0	43.3	48.7
P$_1$A	− 21.9	− 20.0	− 20.6	− 17.2
TS$_1$A-*syn*	43.6	44.0	45.1	49.8
TS$_1$A-*anti*	46.4	47.0	47.2	52.2
IA-*syn*	7.9	8.2	12.6	16.6
TS$_i$A	15.0	14.3	18.0	21.1
IA$_1$-*anti*	11.4	10.9	15.9	19.3
TS$_r$A	14.9	13.6	19.0	21.9
IA$_2$-*anti*	10.2	9.7	14.7	16.0
TS$_2$A	40.1	40.3	39.4	43.7
P$_2$A	− 20.2	− 18.7	− 19.0	15.7
TS$_P$A	− 14.6	− 13.9	− 14.3	− 11.8

[a] Including ZPVE correction from B3LYP/6-31G** frequencies. [b] Single-point calculations on MP2/6-31G** geometries. [c] Single-point calculations on B3LYP/6-31G** geometries.

different bonds across C=C double bonds[22] as a consequence of the amide resonance. The computed bond distances for the forming and breaking C–N bonds at **TS$_c$A** (around 1.65 and 1.81 Å, respectively) characterize this TS as a tight structure in which the new C(azetidinone)–N(NH_3) bond is practically formed, whereas the four membered cycle is barely opened. The transition vector at **TS$_c$A** consists basically of the motion of the hydrogen atom between the two nitrogen atomic centers. The

Table 2. Changes in the B3LYP/6-31G** occupation numbers of the frontier Kohn-Sham orbitals of 2-azetidinone and *N*-methylacetamide in the corresponding $\mathbf{TS_c}$ and $\mathbf{TS_1}$ structures for the ammonolysis and aminolysys reaction. $\Delta\nu$ stands for the net Mulliken charge transfer from amine to amide. The interaction ΔE_{int} and distortion ΔE_{dis} energetic components of the B3LYP/6-31G** energy barriers are also indicated in kcal mol^{-1}.

	Amide				Amine		$\Delta\nu$	ΔE_{int}	ΔE_{dis}		
	NNHOMO	NHOMO	HOMO	LUMO	HOMO	LUMO			Total	NH_3	Amide
NH_3+2-azetidinone											
TS_cA	−0.01	−0.14	−0.13	0.65	−0.49	0.25	0.26	−22.8	66.2	17.8	48.4
TS_1A-*syn*	−0.17	−0.10	−0.02	0.70	−0.52	0.27	0.27	−8.8	53.6	19.6	34.0
TS_1A-*anti*	−0.16	−0.18	−0.01	0.60	−0.43	0.32	0.15	−5.6	53.1	28.3	24.8
NH_3+*N*-methyl-acetamide											
TS_cB	0.00	−0.24	−0.08	0.62	−0.46	0.33	0.19	−24.0	72.0	29.2	42.8
TS_1B-*syn*	−0.19	−0.10	−0.03	0.64	−0.48	0.28	0.22	−3.5	51.3	22.5	28.8
2-azetidinone+methylamine											
TS_cC-*trans*	−0.01	−0.14	−0.14	0.70	−0.52	0.24	0.30	−30.5	69.8	14.5	55.4
TS_1C-*syn*	−0.17	−0.11	−0.04	0.74	−0.54	0.29	0.26	−14.7	55.7	20.4	35.5

MP2/6-31G** energy barrier corresponding to this concerted TS is 47.6 kcal mol^{-1} with respect to the initial **CA** complex (49.3 kcal mol^{-1} at B3LYP/6-31G** level).

The 3-amino-propanamide structure formed by the concerted mechanisms ($\mathbf{P_1A}$ in Figure 1) presents an intramolecular H-bond between the amino and amide groups (NH···N 2.03 Å). The MP2/6-31G** and B3LYP/6-31G** reaction energies for the ammonolysis reaction of 2-azetidinone are −21.9 and −20.6 kcal mol^{-1}, respectively. These values predict an important thermodynamic driving force for the ammonolysis reaction. Taking into account the isodesmic character of the ammonolysis reaction of β-lactams, most of this reaction energy is expected to result from the release of the strain energy of the four-membered ring (see below).

Stepwise mechanism: reversed stereoelectronic control in the formation of the tetrahedral intermediates: **CA** may also evolve through a TS for the 1,2 addition of an ammonia N−H bond across the C=O double bond. Two stereoisomers of this TS were studied in order to discuss the direction of nucleophilic attack (*syn* periplanar or *anti* periplanar with respect to nitrogen lone pair of 2-azetidinone, see **TS_1A-*syn*** and **TS_1A-*anti*** in Figure 1). In contrast with the theory of stereoelectronic control,[23] our calculations render the *syn* periplanar stereoisomer 2.8 kcal mol^{-1} and 2.1 kcal mol^{-1} more stable than the *anti* periplanar one at MP2/6-31G** and B3LYP/6-31G** levels, respectively. According to our analysis, the reason for this energy difference seems to be that the nucleophilic attack of the ammonia molecule displaces the electron lone pair at the nitrogen atom that was originally conjugated with the C=O double bond, forcing it to the *syn* position in which the conjugation is appreciably broken. In effect, in Figure 2 we see that in the *anti* periplanar stereoisomer of **TS_1A-*anti*** there is an important conjugation over the N-C-O part of the β-lactam system, whereas in the *syn* periplanar stereoisomer of **TS_1A-*syn*** this conjugation is clearly diminished. Although this loss of conjugation destabilizes the 2-azetidinone moiety at **TS_1A-*syn***, it also results in a more important ammonia →2-azetidinone charge transfer at **TS_1A-*syn*** that at **TS_1A-*anti***, determining the preferential stabilization of the former structure (see ΔE_{int} and $\Delta\nu$ in Table 2). As a consequence, in the syn periplanar stereoisomer the new C−N bond is more advanced and the carbonyl double bond as well as the endocyclic C−N bond are longer than in the *anti* periplanar one (see Figure 1). The calculated energy barriers with respect to the initial complex for **TS_1A-*syn*** are 48.1 and 49.1 kcal mol^{-1} at the MP2/6-31G** and B3LYP/6-31G** levels, respectively.

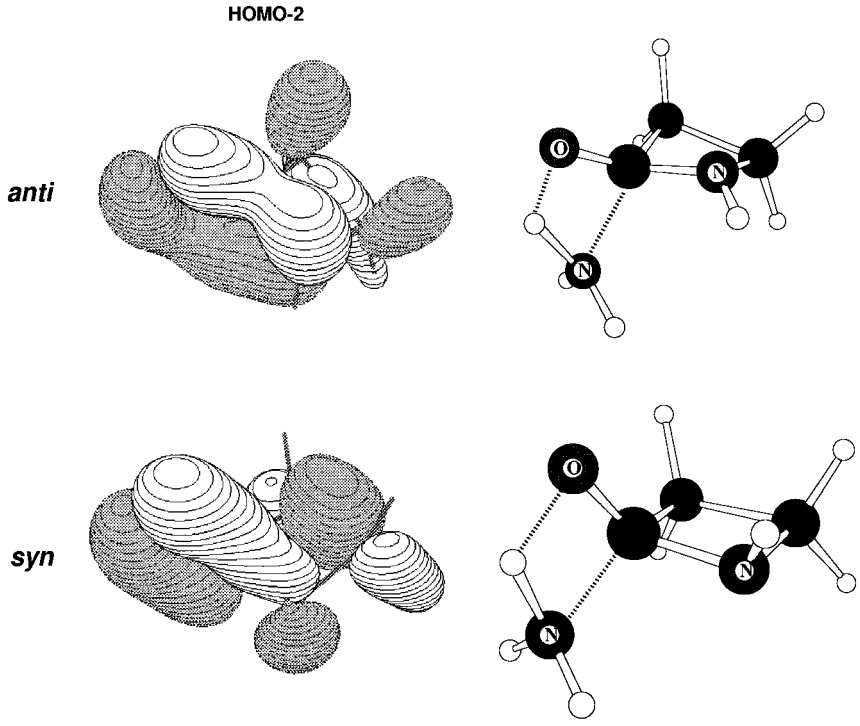

Figure 2. Computer plot of HOMO-2 of distorted 2-azetidinone for the **TS_1A-*syn*** and **TS_1A-*anti*** structures.

TS_1A-*syn* and **TS_1A-*anti*** lead respectively to the stable inter-

0947-6539/99/0503-1048 $ 17.50+.50/0 *Chem. Eur. J.* **1999**, *5*, No. 3

mediates **IA-*syn*** and **IA_1-*anti*** (see Figure 1) in which the C–N endocyclic bond is only slightly elongated, and the four-membered ring has lost its planarity given that the carbonylic carbon atom becomes a tetrahedral center. Again the *syn* periplanar stereoisomer intermediate is 3.5 and 3.3 kcal mol^{-1} more stable than the *anti* periplanar one according to MP2/6-31G** and B3LYP/6-31G** calculations, respectively. The *syn* periplanar intermediate is 12.4 and 16.2 kcal mol^{-1} less stable than **CA** complex at those theory levels. **IA-*syn*** is connected with **IA_1-*anti*** through a TS for the inversion at the nitrogen atom in the four-membered ring, which presents a moderate energy barrier of 7.1 (MP2/6-31G**) and 5.4 (B3LYP/6-31G**) kcal mol^{-1} with respect to **IA-*syn***. An internal rotation about the C–O bond leads from the **IA_1-*anti*** to **IA_2-*anti*** through **TS_rA** shown in Figure 1; the **IA_2-*anti*** intermediate is the immediate precursor to the 3-propanamide product.

Stepwise mechanism: the cleavage of the β-lactam ring: The ring opening of **IA_2-*anti*** to give the product of the *anti* periplanar addition **P_2A** can take place through a TS (**TS_2A** in Figure 1) in which the hydrogen atom is shifted from the oxygen atom to the nitrogen atom of the β-lactam ring with simultaneous breaking of the endocyclic C–N bond. The DFT method provides a moderately more asynchronous **TS_2A** than the MP2 one (see Figure 1). The energy barriers corresponding to **TS_2A** with respect to **CA** are 44.6 and 43.4 kcal mol^{-1} at MP2/6-31G** and B3LYP/6-31G** levels, respectively. These energy values indicate that **TS_1A-*syn*** is the kinetically controlled TS for the nonconcerted ammonolysis of 2-azetidinone (see Table 1) and that the lifetime of the intermediates **IA-*syn***, **IA_1-*anti*** and **IA_2-*anti*** may be long enough to allow their experimental detection given that more than 30 kcal mol^{-1} are required to produce either the ring opening or the NH_3 elimination.

The details of the ring-opening of the four-membered tetrahedral intermediate **IA_2-*anti*** are of mechanistic interest.[3] The analysis of the B3LYP/6-31G** IRC[21] from **TS_2A** to the intermediate **IA_2-*anti*** and to the product clearly shows that the last step of the nonconcerted mechanism may be regarded as occurring in four consecutive stages as follows: i) the β-lactam ring completely flattens; ii) the C–N bond stretches from ≈1.5 Å to ≈1.9 Å, while a disrotatory movement about the N1–C4 and C2–C3 single bonds occurs (this kind of motion has been suggested[3] to avoid small angle strain); iii) a proton is transferred from the oxygen atom to the amidic nitrogen atom (this motion dominates the reaction coordinate at the TS); iv) the C–N bond completely breaks by a stretching motion, which releases the major part of the strain energy rendering a rapidly descending energy profile down to a very stable product, **P_2A** in Figure 1.

The conformation of the reaction product obtained by the stepwise mechanism **P_2A** is slightly less stable than **P_1A** by about 1.6 kcal mol^{-1} (see Table 1). The intramolecular H-bonding between the amino and carbonylic groups in the conformer **P_2A** has an equilibrium NH···O distance around 0.3 Å longer than the comparable NH···N contact in the conformer **P_1A**. Both **P_1A** and **P_2A** structures are interconnected through **TS_PA**, which is 7.3 and 6.3 kcal mol^{-1} less stable than **P_1A** according to MP2/6-31G** and B3LYP/6-31G** levels, respectively. At **TS_PA** the transition vector corresponds basically to the inversion of the amino group, the internal rotation of the amidic group taking place in a later stage of the reaction coordinate to yield the **P_2A** conformer.

Analysis of the rate-determining TSs of the concerted and stepwise mechanisms: From the data discussed above it can be noted that both the **TS_cA** and **TS_1A-*syn*** TSs have several structural characteristics in common. The formation of the C–N single bond between the attacking NH_3 molecule and the carbonylic carbon atom in 2-azetidinone is clearly advanced (≈1.6 Å), while the proton transfer from ammonia to the forming hydroxyl (**TS_1A-*syn***) or amino (**TS_cA)** groups is far from being completed (see Figure 1). These structural data stress the nucleophilic strength of the NH_3 molecule and suggest a NH_3–azetidinone fragment partition as an appropriate reference point to gain a qualitative understanding of these processes.

To visualize the orbital interactions between the β-lactam and the attacking NH_3 molecule, Figure 3 shows a computer plot of the most important B3LYP/6-31G** frontier orbitals

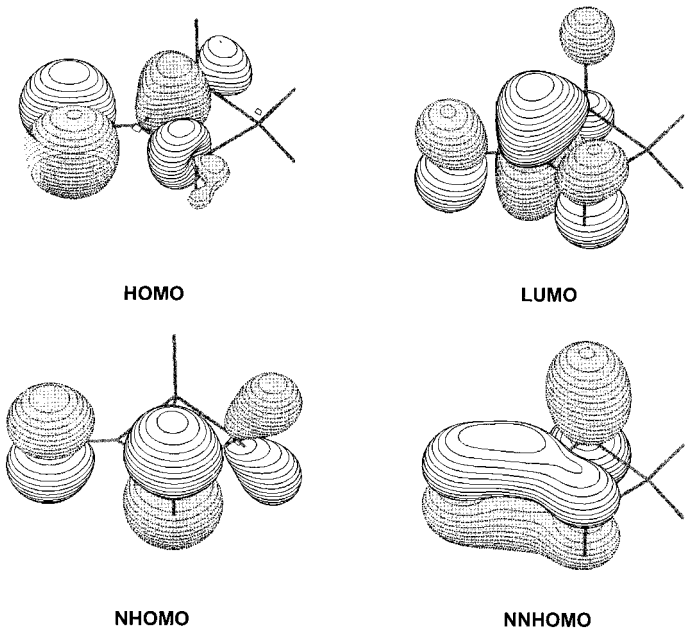

Figure 3. Computer plot of the main frontier MOs involved in the ammonolysis reaction of 2-azetidinone.

of 2-azetidinone. We see in Table 2 that the concerted mechanism is characterized by an important distortion of the β-lactam fragment (48.4 kcal mol^{-1}) and a notable interaction energy between the fragments (−22.8 kcal mol^{-1}). On the contrary, the addition of an ammonia N–H bond across the C=O double bond is favored by a smaller distortion energy of the β-lactam (34.0 kcal mol^{-1}), although the calculated interaction energy between the fragments is only −8.8 kcal mol^{-1}. The charge transfer from NH_3 to the β-lactam does not depend significantly on the bond attacked (C–N or C–O) by the NH_3 molecule as expected from the shape of the LUMO of 2-azetidinone shown in Figure 3. It is interesting to note that the inverse charge transfer from the

amide to NH_3 is markedly different for the attack upon C–N or C–O bonds of 2-azetidinone. Thus, the HOMO (σ_{C-N}) and the NHOMO (N lone pair π_N) of the 2-azetidinone lose 0.13 and 0.14 e at **TS_cA**, respectively, whereas at **TS_1A-*syn*** 2-azetidinone donates 0.10 and 0.17 e from the NHOMO and the NNHOMO (π_{C-O}), respectively.

Interestingly, the rate-determining TSs for the neutral hydrolysis of *N*-methylazetidinone studied by Pitarch et al.[20] have important differences with respect to their corresponding counterparts in the ammonolysis process. In contrast with the discussed **TS_cA** and **TS_1A-*syn*** structures, the proton transfer from H_2O to azetidinone is completed, while the C–O forming bond remains in an initial stage at the TSs for the hydrolysis reaction. The weaker nucleophilic character of water compared with that of ammonia further determines the lack of a *syn* and *anti* periplanar distinction in the stepwise mechanism for the thermal hydrolysis.

High-level energy profiles: Both correlated methods used in this work (MP2/6-31G** and B3LYP/6-31G**) provide similar geometries for the initial complex, intermediates, and TSs located along the reaction coordinate. Furthermore, the corresponding relative energies shown in Table 1 also show that the MP2 and B3LYP energy profiles are readily comparable. Thus, the predicted energy barriers and reaction energies have very similar values, while the B3LYP/6-31G** intermediates are less stable by 4–5 kcal mol^{-1} than the MP2 ones. These energy profiles render the concerted mechanism as the most favorable one by only 0.5 and 1.8 kcal mol^{-1} at the MP2/6-31G** and B3LYP/6-31G** levels, respectively. In view of the small energy differences between **TS_cA** and **TS_1A-*syn***, particularly at the MP2/6-31G** level, we have further investigated the energy profiles at higher levels of theory.

The effect of larger basis set on the energy profiles was first investigated by means of single-point calculations at the B3LYP/6-311 + G(3df,2p)//B3LYP/6-31G** level. In general, a moderate rise of 3–5 kcal mol^{-1} in all the relative energies is observed, so that none of the above discussed trends along the B3LYP/6-31G** reaction profile becomes modified, and the concerted mechanism remains the most favorable one by 1.1 kcal mol^{-1}. When improving both the basis set and the *N*-electron treatment with the G2(MP2,SVP) procedure, the resultant relative energies are not very different from the MP2/6-31G** ones, except in the case of **TS_cA**, which is destabilized by 2.9 kcal/mol (see Table 1). Consequently, at the G2(MP2,SVP) level the stepwise mechanism becomes the most favorable one. **TS_1A-*syn*** is now 2.0 kcal mol^{-1} more stable than **TS_cA** and presents an energy barrier of 47.3 kcal mol^{-1}. It is interesting to note that in contrast with ammonolysis, the neutral hydrolysis of *N*-methyl-2-azetidinone is theoretically predicted to proceed through a concerted mechanism.[20]

The effect of strain energy: The B3LYP/6-31G** and MP2/6-31G** equilibrium structures, located along the concerted and stepwise reaction paths for the ammonolysis reaction of *N*-methyl-acetamide (**CB**, **TS_cB**, **TS_1B-*syn***, etc.), and their relative energies are presented as Supporting Information. These structures are quite similar to those found for the ammonolysis of 2-azetidinone. In this subsection we present only a brief comparative analysis of the ammonolysis of 2-azetidinone and *N*-methyl-acetamide in order to discuss the most important kinetic and thermodynamic effects of strain energy in the ammonolysis of β-lactams.

The energy barrier with respect to the initial complex for the concerted ammonolysis of *N*-methylacetamide is 4.0 (MP2) and 5.1 kcal mol^{-1} (B3LYP) greater than that for 2-azetidinone. The rate-determining TS of the stepwise energy profile is also less stable for the open-chain system by about 2 kcal mol^{-1}. The most remarkable difference between the energy profiles for both ammonolysis reactions is the reaction energy. The ammonolysis of *N*-methylacetamide to give the isolated methylamine and acetamide products is endoergic by 5.6 and 4.4 kcal mol^{-1} according to MP2 and B3LYP methods, respectively. The energy difference between acetamide+CH_3NH_2 and **P_1A** (30.8 kcal mol^{-1}, at MP2/6-31G** level without including the B3LYP/6-31G** ZPVE correction) may be interpreted as due to the strain energy of the four-membered cycle of β-lactams that is released at the final stage of the reaction. In effect, the strain energy of 2-azetidinone computed through the homodesmic reaction shown in Scheme 2 amounts to 28.9 kcal mol^{-1} at the MP2/6-31G** level without including ZPVE energy. This computed strain energy, which is in agreement with the experimental determination[24] of strain in 2-azetidinone ($\Delta H^o = 28.5 \pm 1.4$ kcal mol^{-1}), shows that the release of the strain energy of 2-azetidinone is the main thermodynamic factor favoring its ammonolysis.

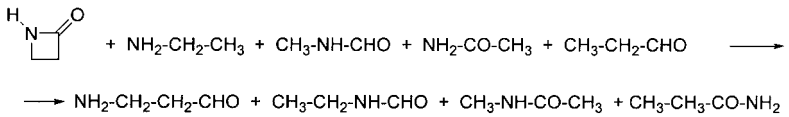

Scheme 2. Homodesmic reaction used to compute the strain energy of 2-azetidinone.

In spite of the important strain energy of 2-azetidinone, it is interesting to note that its kinetic influence is quite moderate. Table 2 shows that the difference in distortion energies at the TSs for the ammonolysis of 2-azetidinone and *N*-methylacetamide is small, and even 2-azetidinone is about 5 kcal mol^{-1} more distorted than *N*-methylacetamide. This fact supports the conclusion that in the ammonolysis of 2-azetidinones no significant release of strain energy occurs along the reaction coordinate until the fourth phase in the opening of the ring at **TS_2A** is passed (see above).

Aminolysis reaction of 2-azetidinone: Figure 4 shows the optimized structures for the aminolysis reaction between 2-azetidinone and methylamine both in gas-phase and in solution. The relative energies of these structures are reported in Table 3. The optimized structures in solution were studied by means of MP2/6-31G** SCRF calculations with a dielectric constant of 78.3 in order to simulate the electrostatic role of

0947-6539/99/0503-1050 $ 17.50+.50/0 *Chem. Eur. J.* **1999**, *5*, No. 3

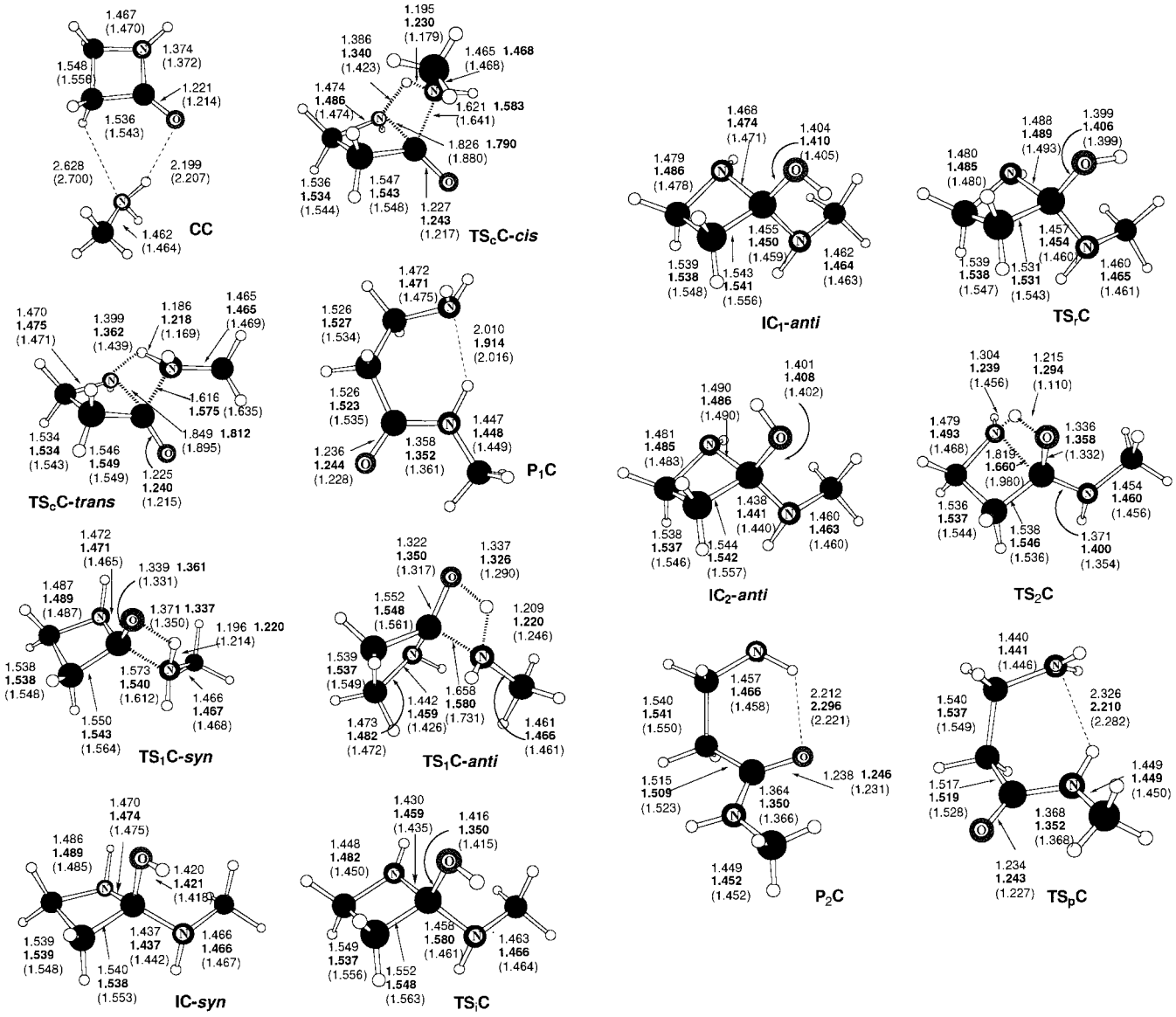

Figure 4. MP2/6-31G**-optimized structures for the aminolysis reaction of 2-azetidinone. Distances in Å. MP2/6-31G** SCRF ($\varepsilon = 78.3$) and B3LYP/6-31G** values are shown in boldface and in parentheses, respectively.

water as solvent. As already mentioned, analogous concerted and stepwise mechanisms have been found for the aminolysis and ammonolysis reactions of 2-azetidinone.

Gas-phase calculations: steric and electronic effects of the methyl group: As in the ammonolysis, the first critical structure located both the concerted and stepwise mechanisms for the aminolysis of 2-azetidinone is the van der Waals complex **CC**. This complex is about 6 kcal mol^{-1} more stable than the reactants (see Table 3).

Two different conformers for the TS structure corresponding to the concerted mechanism were considered depending on the *cis* and *trans* relationship presented by the CH_3–NH_2 bond of the attacking methylamine and the CH_2–CO bond in 2-azetidinone (**TS$_c$C-*cis*** and **TS$_c$C-*trans*** in Figure 4). The *trans* orientation is more favorable by 2.1 and 1.6 kcal mol^{-1} at the MP2/6-31G** and B3LYP/6-31G** levels, respectively, most probably as a result of the minimization of the steric repulsion between the methyl group and the endocyclic methylene groups of 2-azetidinone in that conformation. On the other hand, the concerted cleavage of the initial vdW complex through **TS$_c$C-*trans*** requires 40.8 and 43.1 kcal mol^{-1} at MP2/6-31G** and B3LY/6-31G** levels, respectively. These energy barriers are 6.8 and 4.2 kcal mol^{-1} lower than the corresponding values for the ammonolysis process. The product of the concerted aminolysis is the conformer **P$_1$C** in Figure 4, which is 28.0 and 25.1 kcal mol^{-1} more stable than reactants at the MP2/6-31G** and B3LYP/6-31G** levels, respectively. These values are 6.1 and 4.5 kcal mol^{-1} greater in absolute value than those for the ammnolysis.

Regarding the stepwise mechanism we present only the geometries and energies for the less-hindered *trans* structures located along the reaction path (see Table 3 and Figure 4). At the first TS along the pathway, the nitrogen lone pair at 2-azetidinone is more stable in a *syn* periplanar orientation with respect to the attacking amine than in the *anti* periplanar one (see **TS$_1$C-*anti*** and **TS$_1$C-*syn*** in Table 3 and Figure 4). The rate-determining barrier that corresponds to **TS$_1$C-*syn*** is

Table 3. Relative energies[a] [kcal mol^{-1}] with respect to reactants of the structures considered in the aminolysis reaction between methylamine and 2-azetidinone. Geometries were optimized at MP2/6-31G** and B3LYP/6-31G** levels in gas phase and at the MP2/6-31G** SCRF ($\varepsilon = 78.3$) level in solution.

	MP2/6-31G**	MP2/6-31G**[b] SCRF ($\varepsilon = 78.3$)	B3LYP/ 6-31G**	B3LYP/6-311+ G(3df,2p)[d]
CH_3NH_2+ 2-azetidinone	0.0	0.0 (−7.8)	0.0	0.0
CC	−5.2	−2.6[c] (−5.1)	−4.3	−1.8
TS_cC-*cis*	37.7	39.3 (−6.2)	40.4	44.8
TS_cC-*trans*	35.6	37.4 (−5.9)	38.8	43.5
P_1C	−28.0	−29.0 (−5.7)	−25.1	−21.8
TS_1C- *syn*	36.2	36.8 (−7.0)	40.5	44.8
TS_1C-*anti*	39.3	37.0 (−10.0)	43.3	47.8
IC-*syn*	3.6	8.1 (−3.2)	10.4	14.2
TS_tC	10.5	14.6 (−3.6)	15.6	18.7
IC_1-*anti*	6.9	9.2 (−5.5)	13.5	17.0
TS_tC	10.9	12.0 (−6.6)	16.9	18.6
IC_2-*anti*	5.7	7.6 (−4.8)	12.2	15.5
TS_2C	34.3	35.8 (−6.3)	35.1	38.8
P_2C	−25.8	−25.2 (−7.2)	−23.3	−20.1
TS_PC	−20.6	−18.2 (−5.4)	−18.9	−16.7

[a] Including ZPVE correction from B3LYP/6-31G** frequencies. [b] Electrostatic solvation energies (kcal mol^{-1}) are in parentheses. [c] Single point calculation on the gas-phase MP2/6-31G** geometry. [d] Single point calculations on the B3LYP/6-31G** geometries.

6.7 and 4.3 kcal mol^{-1} lower than that of **TS_1A-*syn*** at MP2/6-31G** and B3LYP/6-31G** levels, respectively.

According to the distances of the forming and breaking bonds, the rate-determining TSs for the concerted and stepwise aminolysis are more advanced than those for the ammonolysis (see Figures 1 and 4). This effect is in agreement with the reinforced electron-donor ability of the primary amine with respect to that of ammonia, thus causing a greater stabilization of the TSs by enhancing the charge-transfer interaction between the amine and 2-azetidinone. The population analysis of **TS_cC-*trans*** and **TS_1C-*syn*** in terms of the fragment MOs shown in Table 2, clearly corroborates this electronic effect given that the HOMO of methylamine donates more charge density than that of ammonia and the lowering in the energy barriers corresponds to larger interaction energies. This $CH_3NH_2 \rightarrow$2-azetidinone charge-transfer interaction has a similar weight in both concerted and stepwise pathways, so that methylamine does not alter the energy difference between them as found in the ammonolysis reaction.

TS_1C-*syn* and **TS_1C-*anti*** connect the prereactive complex with the intermediates **IC-*syn*** and **IC_1-*anti***, respectively. As in the ammonolysis, the *syn* intermediate evolves to the *anti* intermediate **IC_1-*anti*** through a TS for the inversion at the endocyclic nitrogen atom. **IC_1-*anti*** is connected with **IC_2-*anti*** through a TS for the internal rotation of the hydroxyl group. Finally, **IC_2-*anti*** gives the product **P_2C** through **TS_2C**. The optimized tetrahedral intermediates and **TS_2C** structures shown in Figure 4 present the most favorable *trans* orientation of the methyl group. The *syn* intermediate (**IC-*syn*** in Figure 4) is 3.3 and 5.2 kcal mol^{-1} more stable than the **IC_1-*anti*** intermediate. According to the relative energies shown in Tables 1 and 4, the tetrahedral intermediates are slightly stabilized due to methyl substitution by about 4 and 2 kcal mol^{-1} at MP2/6-31G** and B3LYP/6-31G** theory levels, respectively. The cleavage of the endocyclic C–N bond in the **IC_2-*anti*** intermediate through **TS_2C** presents an energy barrier with respect to the initial vdW **CC** complex of 39.5 and 39.9 kcal mol^{-1} at MP2/6-31G** and B3LYP/6-31G** levels, respectively. Concerning the reaction energy, the methyl-substituted conformer **P_2C** is stabilized with respect to the nonsubstituted one in 5.6 and 4.3 kcal mol^{-1} at MP2/6-31G** and B3LYP/6-31G** levels, respectively. At the same theory levels, 5.5 and 4.4 kcal mol^{-1} are required to connect **P_2C** with **P_1C** through **TS_PC** (see Figure 4).

To improve the quality of the energy barriers of the rate-determining TSs as well as to further estimate the energy barrier difference between both concerted and stepwise mechanisms, G2(MP2,SVP) calculations were also carried out on the MP2/6-31G** structures of the initial complex **CC,** the isolated reactants, and the corresponding TSs **TS_1C-*syn*** and **TS_cC-*trans***. At that theory level including the B3LYP/6-31G** ZPVE correction, the calculated binding energy of the prereactive complex is −4.0 kcal mol^{-1}, while **TS_1C-*syn*** is 1.7 kcal mol^{-1} more stable than **TS_cC-*trans***, presenting a barrier height of 41.3 kcal mol^{-1}. Thus, according to the G2(MP2,SVP) calculations the aminolysis of 2-azetidinone would evolve preferentially through the stepwise route.

Electrostatic effect of solvent: The electrostatic influence of solvent on the reaction mechanisms for the aminolysis of 2-azetidinone was taken into account by means of MP2/6-31G** SCRF calculations. The resultant optimized geometries and relative energies are also included in Figure 4 and Table 3, respectively.[25] We see in Figure 4 that the solvated TSs are significantly more advanced than the gas-phase ones. For instance, the C(azetidinone)–N(methylamine) bond distance in **TS_cC-*trans*** and **TS_1C-*syn*** goes from 1.616 and 1.573 Å in gas-phase to 1.575 and 1.540 Å in solution, respectively. These structural changes reveal a certain strengthening of the charge-transfer interaction between fragments induced by solvent. The endocyclic C–N bond distance at **TS_2C** is 0.159 Å shorter in solution than in gas-phase, whereas the hydrogen atom is 0.079 Å more transferred to the forming amine group. On the other hand, the geometry of the tetrahedral intermediates and the product are far less affected by the electrostatic interaction with solvent than that of the TSs, and only a slight elongation of polar bonds is observed in solution.

In general, the MP2/6-31G** SCRF ($\varepsilon = 78.3$) electrostatic solvation energy is greater in absolute value for reactants than for the critical structures located along the different mechanisms by 2–4 kcal mol^{-1}, with the exception of **TS_1C-*syn***, **P_2C**, and, particularly, **TS_1C-*anti*** (see Table 3). The solvation energy of **TS_1C-*syn*** and **P_2C** is less than 1 kcal mol^{-1} lower in absolute value than that of reactants, while the corresponding value for **TS_1C-*anti***, which presents the largest dipole moment, amounts to −10.0 kcal mol^{-1}, 2.2 kcal mol^{-1} greater in absolute value than that for reactants. It is also interesting to note that the electrostatic effect of solvent reduces the energy difference between the *syn* and *anti* periplanar conformers of the stepwise rate-determining TS from 3.1 kcal mol^{-1} in gas-phase to 0.2 kcal mol^{-1} in solution. The

0947-6539/99/0503-1052 $ 17.50+.50/0 *Chem. Eur. J.* **1999**, *5*, No. 3

rate-determining TS for the stepwise mechanism **TS_1C-*syn*** is 1.1 kcal mol^{-1} more stabilized by solvent than the concerted one **TS_cC-*trans*** (see solvation energies in Table 3). As a consequence, MP2/6-31G** SCRF ($\varepsilon = 78.3$) calculations render the stepwise mechanism for the aminolysis as the most favorable one in solution, the energy barrier for the rate-determining step being 0.6 kcal mol^{-1} lower than that for the concerted process. Adding the corresponding solvation energies to the above-presented high-level results, the stepwise mechanism is clearly more favorable than the concerted one by 2.8 kcal mol^{-1}. Finally, we note that a more active participation of solvent molecules in the reaction, not modeled by our continuum SCRF calculations, could be possible.

Conclusions

Two different pathways for the ammonolysis of 2-azetidinone through neutral mechanisms were found on the MP2/6-31G** and B3LYP/6-31G** PESs. MP2 and B3LYP levels of theory render nearly coincident structural and energetical features for these processes and predict the concerted route as the most favorable one. However, the stepwise mechanism is predicted to be the most favored route by 2.0 kcal mol^{-1} when the G2(MP2,SVP) energy corrections are included. The H–NH_2 addition to the C2–N bond of 2-azetidinone causes the simultaneous cleavage of the β-lactam ring with a G2(MP2,SVP) energy barrier with respect to a previous vdW complex of 49.3 kcal mol^{-1}. The stepwise mechanism takes place through the H–NH_2 addition to the C–O double bond of 2-azetidinone leading to the formation of tetrahedral intermediates, which are less stable than the initial complex. Interestingly, the most favored TS for this process presents a *syn* relationship between the nitrogen lone pair of 2-azetidinone and the attacking NH_3 molecule in contrast with the common assumptions of stereoelectronic effects. This is well-rationalized in terms of the greater weight of the 2-azetidinone →NH_3 charge transfer in the *syn* orientation than in the *anti* one. The G2(MP2,SVP) energy barrier required to give the *syn* intermediate from the corresponding vdW precursor amounts to 47.3 kcal mol^{-1}. After inversion at the nitrogen atom of the endocyclic amine and internal rotation of the migrating hydrogen atom about the C–O bond, cleavage of an *anti* intermediate takes place accompanied by the intramolecular proton transfer to form the new amino group. Given that the G2(MP2,SVP) energy barrier for this cleavage is 43.6 kcal mol^{-1} with respect to the prereactive complex, the formation of the tetrahedral intermediate is the kinetically controlled step in the nonconcerted mechanism. Inspection of the B3LYP/6-31G** IRC path for the cleavage of the tetrahedral intermediate reveals a sequence of internal motions, that make possible the distortion of the four-membered heterocycle and the migration of proton avoiding the increase in ring strain. At the corresponding TS the proton is almost transferred to the amino group, and the cleavage of the heterocycle proceeds readily through the product channel by means of a simple stretching motion which releases most of the ring strain.

The kinetic and thermodynamic role of the strain energy of 2-azetidinone has also been investigated by comparing the reaction profile for the ammonolysis of *N*-methylacetamide with that of 2-azetidinone. The difference in the reaction energies for both processes can be interpreted as due to the release of the strain energy associated with the four-membered cycle of β-lactams. Comparison of the energy barriers and the distortion energies at the TSs for the ammonolysis of 2-azetidinone and *N*-methylacetamide shows that the strain energy of 2-azetidinone has only a moderate kinetic relevance and is mostly released at the final stage of the reaction.

The MP2/6-31G** and B3LYP/6-31G** PES for the aminolysis reaction between methylamine and 2-azetidinone have also been studied. According to our results, the electron-donor ability of the methyl group in the attacking amine stabilizes all the TSs in about 4–6 kcal mol^{-1} by reinforcing the charge transfer from the amine to the 2-azetidinone. The electrostatic effect of solvent tends to favor the stepwise mechanism, and to reduce the energy difference between the *syn* and *anti* periplanar conformers of the stepwise rate-determining TSs.

Acknowledgments

The authors thank CIEMAT for computer time on the Cray YMP and are grateful to FICIYT (Principado de Asturias) for financial support (PB-MAS96-23). N.D. also thanks FICIYT for a grant (FC-97-BECA-040).

[1] a) M. I. Page, *Acc. Chem. Res.* **1984**, *17*, 144–151; b) M. I. Page, *The Mechanism of Reactions of β-lactams* in *The Chemistry of β-Lactams* (Ed.: M. I. Page), Blackie Academic & Professional, London, **1992**, pp. 129–147; c) B. B. Levine, Z. Ovary, *J. Exp. Medicine* **1961**, *114*, 875–904; d) C. W. Parker, J. Saphiro, M. Ken, H. N. Eisen, *J. Exp. Medicine* **1962**, *115*, 821–838; e) M. Yvon, J. M. Wal, *FEBS Lett.* **1988**, *239*, 237–240; f) M. Yvon, P. Anglade and J. M. Wal, *FEBS Lett.* **1989**, *247*, 273–278; g) M. Yvon, P. Anglade and J. M. Wal, *FEBS Lett.* **1990**, *263*, 237–240.

[2] G. I. Georg, V. T. Ravikumar, *The Organic Chemistry of β-Lactams.* (Ed.: G. I. Georg), VCH, New York, **1993**.

[3] M. I. Page, *Structure-Activity Relationships: Chemical* in *The Chemistry of β-Lactams* (Ed.: M. I. Page), Blackie Academic & Professional, London, **1992**, pp. 79–100.

[4] M. J. Frisch, G. W. Trucks, H. B. Schlegel, P. M. W. Gill, B. G. Johnson, M. A. Robb, J. R. Cheeseman, T. Keith, G. A. Petersson, J. A. Montgomery, K. Raghavachari, M. A. Al-Laham, V. G. Zakrzewski, J. V. Ortiz, J. B. Foresman, C. Y. Peng, P. Y. Ayala, W. Chen, M. W. Wong, J. L. Andres, E. S. Replogle, R. Gomperts, R. L. Martin, D. J. Fox, J. S. Binkley, D. J. Defrees, J. Baker, J. P. Stewart, M. Head-Gordon, C. Gonzalez, J. A. Pople, *Gaussian 94*, Gaussian, Pittsburgh PA, **1995**.

[5] Adapted by D. Rinaldi from D. Rinaldi, R. R. Pappalardo, Quantum Chemistry Program Exchange, Program no. 622, Indiana University, Bloomington, IN, **1992**.

[6] H. B. Schlegel, *J. Comput. Chem.* **1982**, *3*, 214–218.

[7] W. J. Hehre, L. Radom, J. A. Pople, P. von R. Schleyer, *Ab Initio Molecular Orbital Theory*, Wiley, New York, **1986**.

[8] R. G. Parr, W. Yang, *Density Functional Theory of Atoms and Molecules*, Oxford University Press, New York, **1989**.

[9] a) A. D. Becke, *J. Chem. Phys.* **1993**, *98*, 5648–5652; b) A. D. Becke, *Phys. Rev. A.* **1988**, *38*, 3098–3100; c) C. Lee, W. Yang, R. G. Parr, *Phys. Rev. B.* **1988**, *37*, 785–789.

[10] L. A. Curtiss, P. C. Redfem, B. J. Smith, L. Radom, *J. Chem. Phys.* **1996**, *104*, 5148.

  0947-6539/99/0503-1053 $ 17.50+.50/0

[11] a) J. L. Rivail, D. Rinaldi, M. F. Ruiz-López, in *Theoretical and Computational Model for Organic Chemistry*, *NATO ASI Series C*, *Vol 339* (Eds.: S. J. Formosinho, I. G. Csizmadia, L. Arnaut), Kluwer Academic, Dordrecht, **1991**, pp. 79 – 92; b) V. Dillet, D. Rinaldi, J. G. Angyán, J. L. Rivail, *Chem. Phys. Lett.* **1993**, *202*, 18 – 22; c) V. Dillet, D. Rinaldi, J. L. Rivail , *J. Phys. Chem*. **1994,** *98*, 5034 – 5039.
[12] P. Claverie, in *Quantum Theory of Chemical Reactions*, *Vol 3* (Eds.: R. Daudel, A. Pullman, L. Salem, A. Veillard), Reidel, Dordrecht, **1982**, pp. 151 – 175.
[13] H. Fujimoto, S. Kato, S. Yamabe, K. Fukui, *J. Chem. Phys.* **1974**, *60*, 572; b) M. I. Menéndez, J. A. Sordo, T. L. Sordo, *J. Phys. Chem.* **1992**, *96*, 1185 – 1187.
[14] L. Bencivenni, F. Ramondo, J. J. Quirante, *J. Mol. Struct. [Theochem]* **1995**, *330*, 389 – 393.
[15] R. López, M. I. Menéndez, D. Suárez, T. L. Sordo, J. A. Sordo, *Comput. Phys. Commun.* **1993**, *76*, 235 – 249.
[16] J. P. Krug, P. L. A. Popelier, R. F. W. Bader, *J. Phys. Chem.* **1992**, *96*, 7604 – 7616.
[17] J. H. Jensen, K. K. Baldridge, M. S. Gordon, *J. Phys. Chem.* **1992**, *96*, 8340 – 8351.
[18] S. Antonczanck, M. F. Ruiz-López, J. L. Rivail, *J. Am. Chem. Soc.* **1994**, *116*, 3912 – 3921.
[19] S. Wolfe, C.-K. Kim, K. Yang, *Can. J. Chem.* **1994**, *72*, 1033 – 1043.
[20] J. Pitarch, M. F. Ruiz-López, J. L. Pascual-Ahuir, E. Silla, I. Tuñón. *J. Phys. Chem. B.* **1997**, *101*, 3581 – 3588.
[21] a) K. Fukui, *Acc. Chem. Res.* **1981**, *14*, 363 – 375; b) C. González, H. B. Schlegel, *J. Phys. Chem*. **1990**, *94*, 5523 – 5527.
[22] M. I. Menéndez, D. Suárez, J. A. Sordo, T. L. Sordo, *J. Comput. Chem*. **1995**, *16*, 659 – 666.
[23] P. Deslongchamps, *Stereoelectronic Effects in Organic Chemistry*, Pergamon, Oxford, **1983**.
[24] M. V. Voux, P. Jiménez, J. Z. Dávalos, O. Castaño, M. T. Molina, R. Notario, M. Herreros, J.-L. M. Abboud, *J. Am. Chem. Soc*. **1996**, *118*, 12735 – 12737.
[25] The optimization of the vdW structure **CC** in solution was not possible as a consequence of the inadequacy of the cavity model for weak intermolecular complexes. A single-point calculation on the gas-phase MP2/6-31G** geometry was performed instead (see Table 3).

Received: March 30, 1998
Revised version: September 7, 1998 [F 1073]

  0947-6539/99/0503-1054 $ 17.50+.50/0